IEEE Access
Multidisciplinary | Rapid Review | Open Access Journal

Received February 18, 2019, accepted May 4, 2019, date of publication May 16, 2019, date of current version June 6, 2019.

*Digital Object Identifier 10.1109/ACCESS.2019.2917317*

# A New Control Method Based on DTC and MPC to Reduce Torque Ripple in SRM

**AIDE XU[1], CHAOYI SHANG[2], JIAGUI CHEN[1], JINGWEI ZHU[2], AND LELE HAN[1]**
[1]College of Information Science and Technology, Dalian Maritime University, Dalian 116026, China
[2]College of Marine Electrical Engineering, Dalian Maritime University, Dalian 116026, China

Corresponding author: Jingwei Zhu (zjwdl@dlmu.edu.cn)

This work was supported in part by the National Natural Science Foundation of China under Grant 51407021, in part by the Fundamental Research Funds for the Central Universities of China under Grant 3132019015, and in part by the Dalian Science Technology Innovation Fund Project under Grant 2018J12GX039.

**ABSTRACT** This paper proposes a new control strategy to reduce torque ripple in a switched reluctance motor (SRM). The flux linkage in this paper is related to model predictive flux control (MPFC). In addition, the torque hysteresis remained in the system is similar to direct torque control (DTC) and direct instantaneous torque control (DITC). The candidate voltage vectors (VVs) are selected from the torque hysteresis and the cost function is designed for the flux linkage minimization to select the best VV from candidate VVs. The advantages, as well as the improvement prospects for these methods, are discussed in details. Performance for torque ripple in steady state and the robustness in the transient state are evaluated in this paper under the simulation and experimental results, and also the possibility and some advice for model predictive control (MPC) applied to an SRM are indicated. The experimental result for the new method is carried out on a three-phase 12/8 poles SRM with the analysis of torque ripple compared to a DTC and DITC.

**INDEX TERMS** Direct torque control, model predictive control, switched reluctance motor.

## I. INTRODUCTION

Switched reluctance motor (SRM) has the advantages of low inertia, fault tolerance, high efficiency, simple design and has been applied to some fields such as hybrid electric vehicle applications, aviation industry, household appliances and so on [1]–[3]. But the shortcomings of the torque ripple have not been well resolved for a long time, which limits the application scope and field of SRM [4]–[6]. The reasons for the large torque ripple are doubly salient structure and highly nonuniform torque magnetization characteristics. This unique characteristic results in different control schemes compared with other motor drive systems such as induction machine (IM) and permanent magnet synchronous motor (PMSM).

In order to solve the problem of the high torque ripple of SRM drive system, many researches have been undertaken over the past few decades. In general, the control strategy can be divided into two broad categories: indirect torque control and direct torque control (DTC). The indirect torque control usually uses current control or torque-shared function (TSF) to coordinate the individual phases and track the command value. In [7], the tracking performance of the reference current is improved, and the current ripple is reduced by changing the position of the current sampling point. In [8], [9] back EMF compensation to the PI current controller has been analyzed. In [10], the TSF is used to coordinate the torque production of individual phases. In [11] four common TSFs based on linear, cubic, sinusoidal and exponential functions are evaluated and optimized to satisfy the primary objective of low torque ripple. The minimization of the copper losses, minimization of the peak phase current and maximized the torque-speed range are studied in [12]–[14]. However these methods require intensive computation, torque-to-current converter and long settling time for the self-tuning of controller parameters, also the dynamic response may not be satisfied.

Direct torque control schemes for SRM can partly overcome these shortcomings. The important feature of DTC is that torque is directly regarded as a control variable and there is no current control loop any more. In [15], direct instantaneous torque control (DITC) method is put forward to solve the torque ripple problem. In [16], direct torque and flux control (DTFC) method is proposed for SRM drives. Based on these methods, several researches to

The associate editor coordinating the review of this manuscript and approving it for publication was Alfeu J. Sguarezi Filho.

reduce torque ripple have been undertaken. In [17], a low cost bus current detection-based DITC scheme for SRM drives under soft-chopping mode is developed. In [18], the DITC algorithm is compared with the current profiling technique using three different TSFs. In [19] the improved DTC method to get better torque-ampere ratio is introduced.

As the discrete nature of the voltage source inverter and limited number of voltage vectors, MPC has gained more attention among the proposed strategies. Some of the most salient features of MPC include being simple to apply in multivariable systems, fast transient response, inclusion of nonlinearities and constraints in the control law is straightforward [20], [21]. For the proposed of the direct torque and flux control, MPC with various strategies appear to be a possible alternative to the traditional DTC scheme [22]. Many scholars have already successfully used this method to control the flux and torque in induction machine and permanent magnet synchronous motor [23]–[27]. Some researches also propose the MPC strategy being used in SRM [28], [29]. In [28], a predictive current control based on deadbeat solution is presented to follow the reference phase current with a fixed switching frequency. In [29], an on-line inductance surface estimator with a stochastic MPC method for SRM is introduced.

Since MPC is a promising method to handle the non-linear magnetic characteristic of SRM and avoid the complex switching rules, this paper presents a strategy based on the DTC and model predictive flux control (MPFC). The torque hysteresis is embedded in the system, and select four candidate VVs among 12 VVs to increase or reduce torque. The cost function is designed for flux linkage minimization. As the cost function only has one variable, the weighting factor is eliminated. This control strategy is compared with 12VVs DTFC and optimized DITC for the performance of torque ripple in steady state and transient state. The advantages as well as the improvement prospects for these methods are discussed in details. Neither IM nor PMSM, the instantaneous torque in SRM mainly depends on the partial derivative of stator flux linkage respect to angle which means there is a first order delay between torque and flux linkage. Using the flux linkage hysteresis will lead to more error to the system especially in torque commutation region. The proposed method uses cost function to exactly track the reference flux and eliminate torque ripple. Some advice for MPC applied to SRM and the necessity to remain the torque hysteresis are also indicated in this paper.

## II. MATHEMATICAL MODEL FOR SRM

### A. TORQUE EQUATION

On the basis of Faradays law, the instantaneous voltage across the terminals of one single phase winding for SRM is shown in (1). Where $U_P$, $i_p$, $\psi_p$, $\theta$, corresponding to the terminal voltage, phase current, winding flux linkage, rotor position. $R$ is the motor winding resistance.

$$U_p = i_p R + \frac{\mathrm{d}\psi_p}{\mathrm{d}t} = i_p R + \frac{\partial \psi(i_p,\theta)}{\partial i_p}\cdot\frac{\mathrm{d}i_p}{\mathrm{d}t} + \frac{\partial \psi(i_p,\theta)}{\partial \theta}\cdot\frac{\mathrm{d}\theta}{\mathrm{d}t} \quad (p = 1, 2, 3) \tag{1}$$

According to (1), the instantaneous one phase torque equation for SRM is inferred in details in literature[17], which can be expressed as:

$$T_p = i_p \frac{\partial \psi_p(\theta, i_p)}{\partial \theta} - \frac{\partial W_f}{\partial \theta} \tag{2}$$

where $W_f$ is the field energy. Due to saturation in the SRM, the influence of the $\partial W_f/\partial\theta_p$ in (2) is very small and can be neglected. The instantaneous torque in SRM is generally expressed as:

$$T_p \approx i_p \frac{\partial \psi(\theta, i_p)}{\partial \theta} \tag{3}$$

Obviously there is a first order delay between torque and flux linkage in SRM. This unique relationship leads to a different control strategy for MPC being used in SRM. Also, the complex torque characteristic is one of the reasons why torque hysteresis is still remained in the proposed method.

### B. FLUX MODEL FOR PROPOSED METHOD

Establishment of an accurate non-linear model of SRM is an important prerequisite for high performance torque control. The locked rotor test is used to obtain the accurate flux model of the SRM. The SRMs' flux linkage character in this paper is shown in Fig. 1(a).

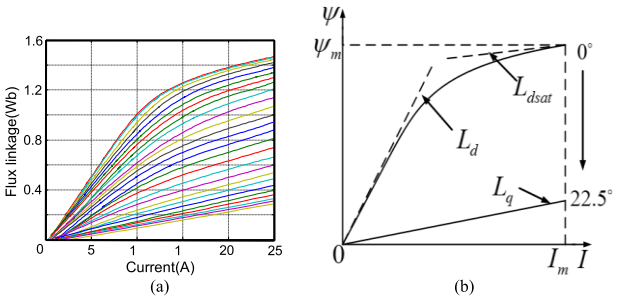


**FIGURE 1.** Flux linkage characters and nonlinear mathematical model.

This paper adopts the nonlinear flux analytical model from [30], because of its clear concept and simple expression. This model neglects the mutual couplings between the phases, and the rotor position on the flux linkage can be separated. Fig. 1(b) shows the principle for this method. The inductance which corresponds to aligned and unaligned rotor positions are obtained from locked rotor test. The expression for this model is shown in (4)-(6).

$$\left\{\begin{array}{l} A = \psi_m - L_{dsat} I_m \\ B = (L_d - L_{dsat})/(\psi_m - L_{dsat} I_m) \\ \psi_d = L_{dsat} i + A(1 - e^{-Bi}) \\ \psi_{\mathrm{q}} = L_q i \end{array}\right\} \tag{4}$$

where $L_d$, $L_{dsat}$, $L_q$ are corresponding to the aligned non-saturated inductance, aligned saturated inductance and unaligned inductance. $A$ and $B$ are constants which determined by conditions at $i = 0$ and $i = I_m$. The magnetization characteristics can be expressed as:

$$\psi(i,\theta) = L_q i + \left[L_{\text{dsat}} i + A(1 - e^{-Bi}) - L_q i\right] f(\theta) \tag{5}$$

$$f(\theta) = \begin{cases} \dfrac{1024(\frac{\pi}{8} - \theta)^3}{\pi^3} - \dfrac{192(\frac{\pi}{8} - \theta)^2}{\pi^2} + 1 & \theta \in [0, \dfrac{\pi}{8}] \\ f(\dfrac{\pi}{4} - \theta) & \theta \in [\dfrac{\pi}{8}, \dfrac{\pi}{4}] \end{cases} \tag{6}$$

### C. CONVERTER TOPOLOGY AND SECTOR PARTATION

The converter topology for SRM is shown in Fig. 2. The combination of three-phase switching states is described as a switching vector Sg = [s1 s2 s3], which means there are 27 switching vectors as the control signal applied to the power converter in each sampling time. When Sg = 1, two switches on the same bridge arm are turned on at the same time and the voltage added to the winding is +Udc. When Sg = 0, one of the switches is turned on and another is turned off, the current freewheels through the diode, and the voltage added to the winding is zero. When Sg = −1 two switches are both turned off, the current flows through the two diodes and the voltage added to the winding is –Udc. The corresponding switch state for VVs and the sector partition are shown in Fig. 3.

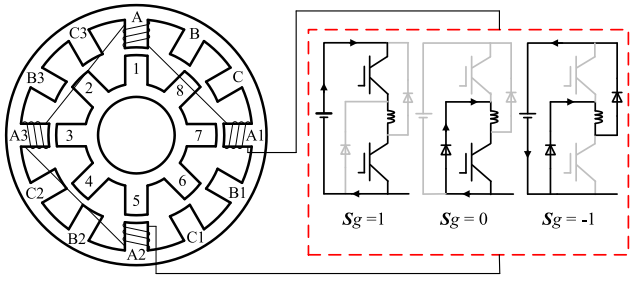


**FIGURE 2.** SRM with asymmetric bridge converter.

## III. OPERATION PRINCIPLE

### A. SELECTING RULE FOR VOLTAGE VECTOR

As mentioned before, the torque hysteresis is remained in the proposed method, and there are 12 sectors which are divided by 12 VVs in this paper. The function for torque hysteresis is to select the candidate VVs for cost function to increase or decrease the torque based on current sector. For instance, if the stator space vector lies in sector one, $\vec{v}_2$, $\vec{v}_3$, $\vec{v}_4$ and $\vec{v}_5$ can increase the torque, correspondingly $\vec{v}_8$, $\vec{v}_9$, $\vec{v}_{10}$ and $\vec{v}_{11}$ can decrease the torque. This principle is quite similar to the DTC strategy. In sector one, $\vec{v}_1$, $\vec{v}_6$ and $\vec{v}_7$, $\vec{v}_{12}$ can also increase or decrease the torque, but these four VVs are in the critical position, which means they have very small effect in torque and large effect in flux linkage. Since the other 8 VVs can totally satisfy the need to control the torque, in order to increase the system robustness, the VVs

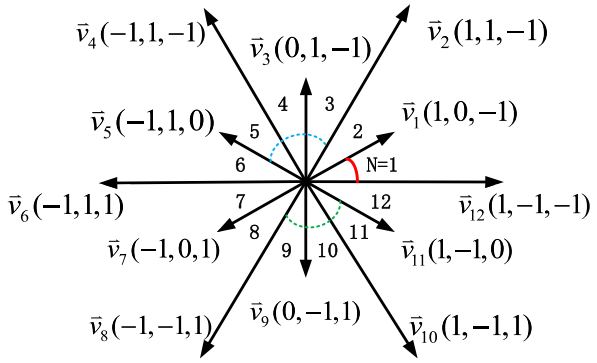


**FIGURE 3.** Voltage vector and sector partition.

**TABLE 1.** Candidate voltage vectors selection table.

| Sector / Signals | 1 | 2 | 3 | 4 |
|---|---|---|---|---|
| $T_+$ | $\vec{v}_{2,3,4,5}$ | $\vec{v}_{3,4,5,6}$ | $\vec{v}_{4,5,6,7}$ | $\vec{v}_{5,6,7,8}$ |
| $T_-$ | $\vec{v}_{8,9,10,11}$ | $\vec{v}_{9,10,11,12}$ | $\vec{v}_{10,11,12,1}$ | $\vec{v}_{11,12,1,2}$ |
| **Sector / Signals** | **5** | **6** | **7** | **8** |
| $T_+$ | $\vec{v}_{6,7,8,9}$ | $\vec{v}_{7,8,9,10}$ | $\vec{v}_{8,9,10,11}$ | $\vec{v}_{9,10,11,12}$ |
| $T_-$ | $\vec{v}_{12,1,2,3}$ | $\vec{v}_{1,2,3,4}$ | $\vec{v}_{2,3,4,5}$ | $\vec{v}_{3,4,5,6}$ |
| **Sector / Signals** | **9** | **10** | **11** | **12** |
| $T_+$ | $\vec{v}_{10,11,12,1}$ | $\vec{v}_{11,12,1,2}$ | $\vec{v}_{12,1,2,3}$ | $\vec{v}_{1,2,3,4}$ |
| $T_-$ | $\vec{v}_{4,5,6,7}$ | $\vec{v}_{5,6,7,8}$ | $\vec{v}_{6,7,8,9}$ | $\vec{v}_{7,8,9,10}$ |

in the critical position for every sector are eliminated from the candidate VVs. The torque hysteresis only select four VVs for cost function in every sampling time to increase or decrease the torque. The candidate VVs selection table is listed in Table 1. Since the torque and flux linkage are controlled separately, the uphill task to find the best weighting factor in cost function can be eliminated.

### B. PRINCIPLE FOR THE PROPOSED METHOD

In order to get the flux linkage in the next period, the current in the next period need to be predicted. The dynamics of the current and the angular velocity are shown as follow:

$$\frac{di_P}{dt} = \frac{1}{\partial\psi_P/\partial i_P}\left[U_P - Ri_P - \frac{\partial\psi_P}{\partial\theta}\omega\right] \quad \frac{d\theta}{dt} = \omega \tag{7}$$

Based on normal forward Euler approximation, the prediction of stator current at next control period $i(k+1)$ can be expressed as:

$$i_p(k+1) = i_p(k) + \frac{T_s}{\partial\psi_p(k)/\partial i_p(k)}[U_p(k) - Ri_p(k) - \frac{\partial\psi_p(k)}{\partial\theta(k)}\omega(k)] \tag{8}$$

where $T_s$ is the control period and $i_p(k+1)$ is the phase current in the next period. $U_p(k)$ is corresponds to the candidate VVs which are selected by the torque hysteresis. The flux linkage at $k+1$ period can be calculated from (9).

$$\psi_p(k+1) = L_q i_p(k+1) + f(\theta(k+1))\left[L_{\text{dsat}} i_p(k+1) + A(1-e^{-Bi_p(k+1)}) - L_q i_p(k+1)\right] \quad (9)$$

The cost function can be expressed as:

$$\text{g} = ||\psi(ref)| - |\psi(k+1)|| \quad (10)$$

The optimum voltage vector is selected based on flux linkage minimization from (10), and the corresponding switching state is applied to the converter.

As there is only one parameter in the cost function, the weighting factor can be eliminated. The expression for cost function in traditional MPC is shown in (11). Where $\lambda_\psi$ is the weighting factor for stator flux [20], [21].

$$\text{g}_1 = |T_\text{e}(ref) - T_\text{e}(k+1)| + \lambda_\psi \, ||\psi(ref)| - |\psi(k+1)|| \quad (11)$$

Several methods have been adopted to obtain a proper weighting factor [31]–[33]. These methods have been proved to be effective, but since different variables are added in the cost function, the task to find the most suitable weighting factor for those variables become complicated. For different machines, structures and conditions, the value of the best weighting factor may also change. So the advantage of removing weighting factor is obvious. The control diagram of the proposed algorithm is shown in Fig. 4.

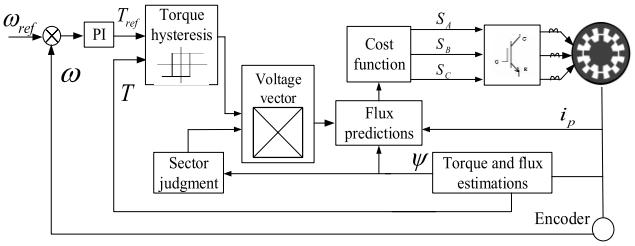


**FIGURE 4.** Control diagram.

The flowchart is shown in Fig.5. In conclusion, the proposed method can be applied in the following steps:

1) Measure the stator current, rotor speed, rotor position, and dc-link voltage;
2) Estimate the valve of stator flux and electrical torque at $k$ period;
3) Select four VVs based on the comparison between $T_e(ref)$ and $T_e(k)$ in torque hysteresis;
4) Predict the stator current and flux linkage at $k+1$ period;
5) Use the cost function to select the optimum voltage vector from four candidate VVs based on flux linkage minimization;
6) Send the corresponding switching states to three phase asymmetric bridge converter.

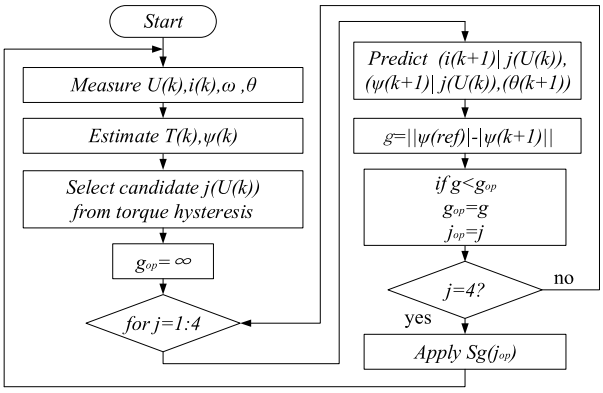


**FIGURE 5.** Flowchart for proposed algorithm.

## IV. INNOVATION AND COMPARISION

### A. COMPARISION WITH DTC

DTC has already been proposed for many years which covers three-phase, four-phase and also six-phase SRMs. The improvement for this method is focused on VVs optimization. Increase the number of candidate vvs is the most popular way to improve DTC. from (3), it is easy to know that the torque changes behind the flux linkage, the variation in torque at current period is caused by the variation in flux linkage last period. But for DTC, the torque hysteresis and flux hysteresis select the VVs at the same time under the same coordinate, which means the first order delay between torque and flux linkage in SRM is neglected. And the nonlinear electromagnetic characteristic for SRM will result in more errors to this double hysteresis system in commutation zone as a sudden increase for the positive torque and a sudden decrease for the negative torque. Additionally, in theory hysteresis can only control the variable varies within the band width, which means the range of the hysteresis band is very important. For proposed method, as the flux hysteresis is replaced by cost function, the flux linkage can be controlled in advance to reduce torque ripple. The proposed method is compared with 12 VVs DTC and optimized DITC in the following part.

### B. COMPARISION WITH MPC

In the former research, MPC is adopted directly in SRM just like other motors, the cost function consists torque, flux linkage and even switching frequency in simulation. As mentioned before, from (2), it is easy to know that the torque characteristic in SRM is complicated. Fig. 6 shows the torque characteristic obtained from experimental result. In traditional MPC method for IM or PMSM, the torque could be expressed accurately with mathematical formulas. But for SRM, whether to use nonlinear flux model indirectly calibrated or use mathematical model to describe directly, the accuracy may not be satisfied for practical implementation. Because the torque and flux characteristic cannot be expressed under the same model, remaining the torque hysteresis is vital for the control system as it permits independent control of torque and flux linkage.

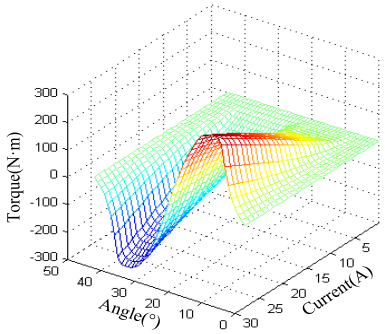


**FIGURE 6.** Torque characteristics.

Additionally, remaining torque hysteresis can get better dynamic performance, conquer the influence of model error and simplify the algorithm.

## V. IMPLEMENTION AND RESULT

### A. SIMULATION RESULTS

To verify the effectiveness for the proposed schemes, simulations are performed in MATLAB/Simulink. The parameters of the SRM are given in Table 2. And the control parameters for simulation are listed in Table 3. Both DTC and proposed method are executed under 12 VVs. The turn on/off angle for DITC are optimized under different conditions and the hysteresis rules are optimized from [38].

**TABLE 2.** Parameters of the SRM.

| Parameter | Value | Parameter | Value |
|---|---|---|---|
| Outer diameter of the stator | 258 mm | Inner diameter of the stator | 160 mm |
| Outer diameter of the rotor | 159 mm | Inner diameter of the stator | 83 mm |
| Stator resistance | 0.6 Ω | Stator/rotor poles | 12/8 |
| Stator core length | 184.3 mm | Air-gap | 1 mm |
| Unaligned inductance | 11.44 mH | Stator slot depth | 27 mm |
| Aligned inductance | 104.30 mH | Rotor slot depth | 23 mm |
| Stator yoke height | 22 mm | Rotor yoke height | 15 mm |

**TABLE 3.** Control parameters.

| Parameter | Value |
|---|---|
| Reference speed | 800 r/min |
| Torque load | 5→15 N•m |
| Given torque | 20 N•m |
| Bandwidth of torque hysteresis loop (DTC/proposed method) | ±0.2 N•m |
| Bandwidth of torque hysteresis loop (DITC) | ±0.2 N•m/ ±0.25 N•m |
| Bandwidth of flux hysteresis loop (DTC) | ±0.01 N•m |
| Reference flux | 0.33 Wb |

The simulation results of DTC, proposed method and DITC are shown in Fig. 7. The flux circles for these schemes are shown in Fig. 8 and Fig. 9 shows the phase current, total torque and real time sector zone. From the simulation result, as the turn on/off angle and hysteresis rules for DITC

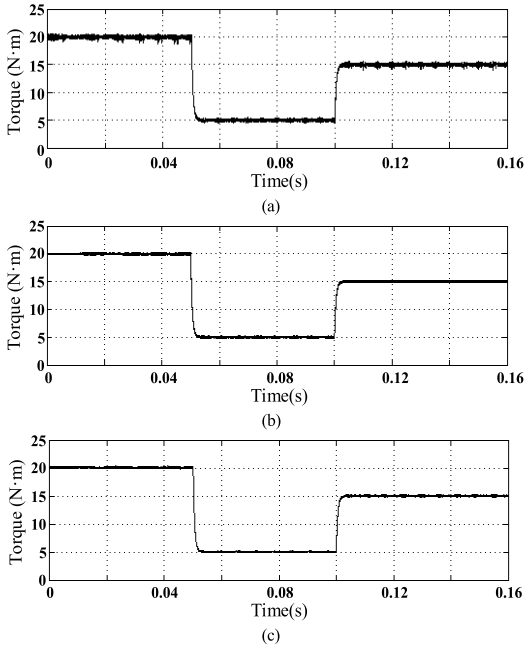


**FIGURE 7.** Torque ripple overall process. (a) DTC. (b) Proposed method. (c) DITC.

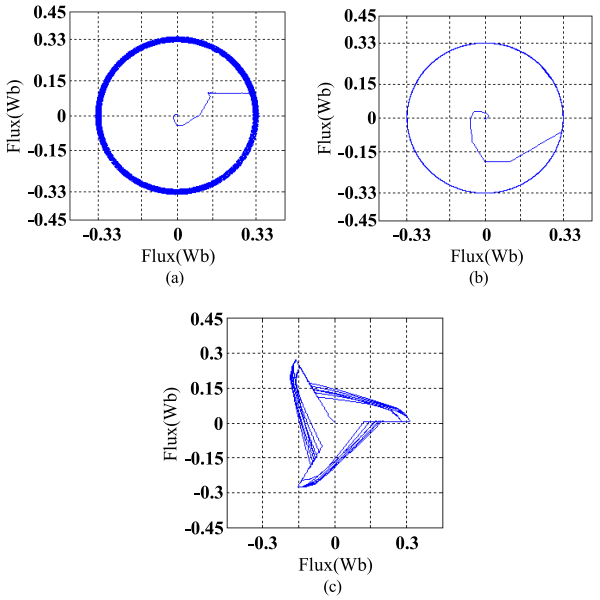


**FIGURE 8.** Flux linkage circle overall process. (a) DTC. (b) Proposed method. (c) DITC.

are optimized, the distinction between DITC and proposed method is fairly small. And the effect for 12VVs DTC method is only a third of the other two methods. The influence of different turn on/off angles for the torque ripple in DITC is shown in Fig. 10.

### B. EXPERIMENTAL RESULTS AND ANALYSIS

Fig. 11 shows the platform for the locked rotor test. Fig. 12 presents the recorded phase current and voltage of A-phase at the aligned position (22.5°) and unaligned position (0°).

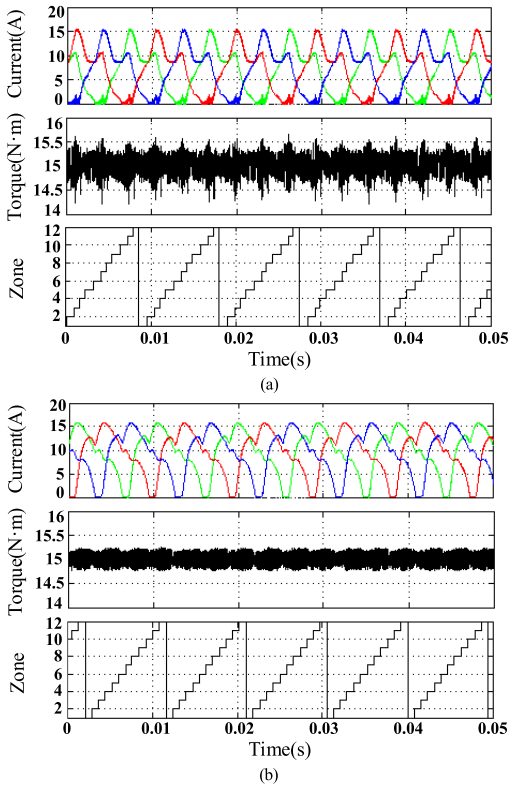


**FIGURE 9.** 800r/min with 15N-m load. (a) DTC. (b) Proposed method.

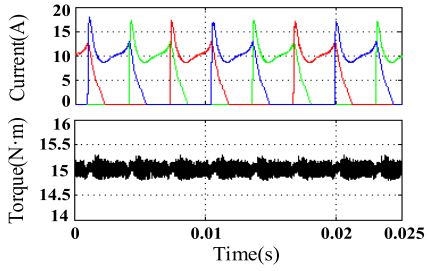


**FIGURE 10.** Optimized DITC with 15N-m load and 800r/min.

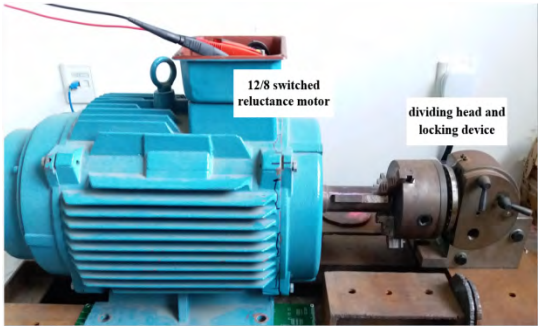


**FIGURE 11.** Platform for the locked rotor test.

Fig. 13(a) shows the original data for magnetization curves based on one locked rotor test. Compared with the magnetization curves for analytical nonlinear functions which is shown in Fig. 13(b), it can be found that the maximum deviation

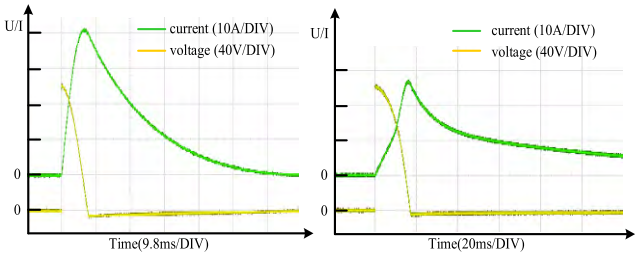


**FIGURE 12.** Current and voltage of phase A at 0° and 22.5°.

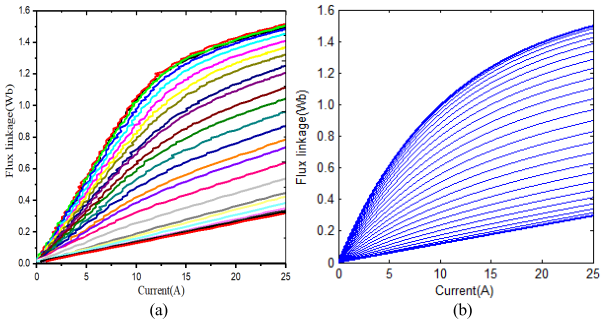


**FIGURE 13.** Magnetization curves. (a) Locked rotor test. (b) Analytical nonlinear functions.

**TABLE 4.** Key elements specification.

| Key Elements | Key Parameters | Value |
|---|---|---|
| Intelligent power module | Maximum of frequency(KHz) | 20 |
| Encoder | Absolute position signal | 1024 |
| TMS320F2812 | Main frequency(MHz) | 120 |
| Magnetic powder brake | Maximum of braking torque(N • m) | 50 |
| Oscilloscope | Band width (MHz) | 200 |
| | Max Samples (GSa/s) | 5 |
| Current sensor | Supply voltage(V) | ±12 to 15(±5%) |
| | Accuracy | ±0.5% |
| Voltage sensor | Supply voltage(V) | ±12 to 15(±5%) |
| | Accuracy | ±0.7% |
| Torque speed sensor | Torque accuracy(F • S) | 0.1—0.5% |
| | Repeatability(F • S) | 0.1—0.5% |
| | Linearity(F • S) | 0.1—0.5% |
| | Lag(F • S) | 0.1—0.5% |
| | Output frequency signal amplitude (V) | 5 |

between calculated and measured flux linkage characteristics is less than 10%. Moreover, from the perspective of the entire control algorithm, as the torque hysteresis only selects 4 candidate VVs, comparing to the impact of the VVs per period on the flux linkage, this nonlinear model can be used to predict the future states of the system. The platform consists of distinct subsystems, including a three-phase IPM converter, a DSP controller, a 12/8 pole three-phase SRM and the interfaces for signal input and output. In this paper, the control

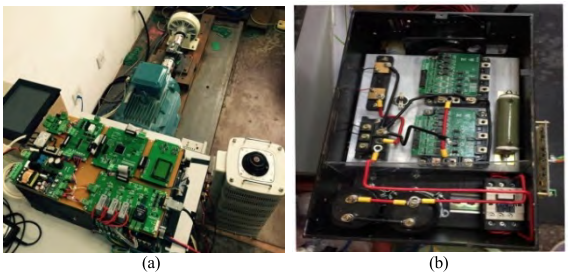


**FIGURE 14.** Hardware test platform. (a) All system. (b) Converter.

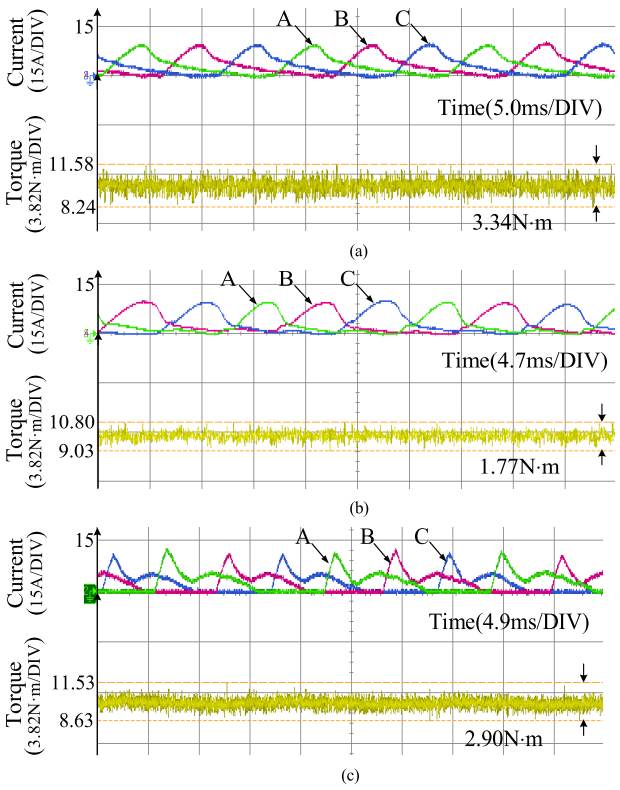


**FIGURE 15.** 450r/min with 10N · m load torque. (a) DTC. (b) Proposed method. (c) DITC.

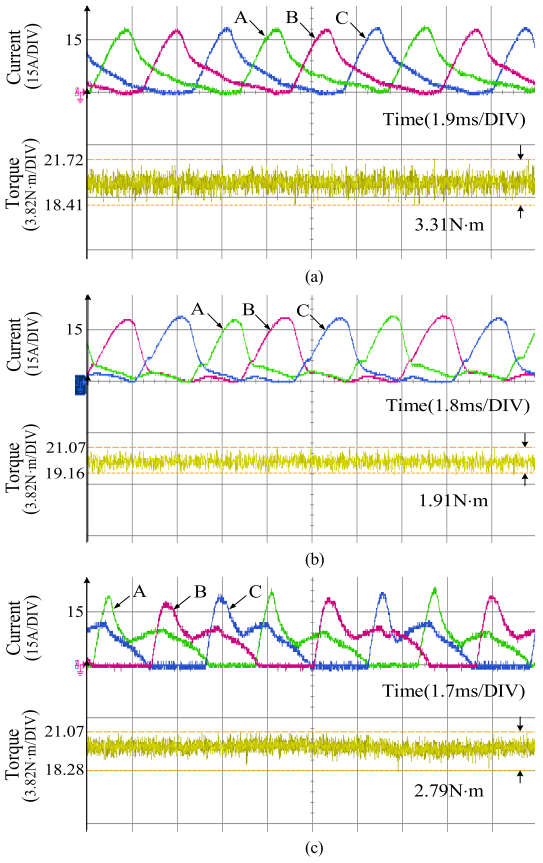


**FIGURE 16.** 1200r/min with 20N · m load torque. (a) DTC. (b) Proposed method. (c) DITC.

**TABLE 5.** Torque ripple coefficient for each methods.

| Method | 450r/min 10N•m | 1200r/min 20N•m |
|---|---|---|
| DTC (12VVs) | $T_{RC}$=3.34 | $T_{RC}$=3.31 |
| Proposed method | $T_{RC}$=1.77 | $T_{RC}$=1.91 |
| DITC (optimized angle) | $T_{RC}$=2.90 | $T_{RC}$=2.79 |

period for each method is 83$\mu$s, magnetic powder brake is adopted as the load torque of SRM and the oscilloscope is used to measure the output signal from torque sensor. The specification for the sensors are shown in Table 4 and the hardware test platform is shown in Fig. 14.

Fig. 15 and Fig. 16 show the three-phase current waveform and torque ripple under 450rpm with 10N · m load torque and 1200rpm with 20N · m load torque. Similar to the simulation, the proposed method is compared to 12VVs DTC and optimized DITC.

In order to quantify the concentration of torque for these methods, the torque standard deviation $T_{std}$ and torque ripple coefficient $T_{RC}$ are adopted as evaluation index.

$$T_{std} = \sqrt{\frac{\sum_{i=1}^{n}(T_e - T_{av})^2}{n}} \qquad T_{RC} = T_{\max} - T_{\min} \tag{12}$$

where $n$ is the number of samples, $T_e$ is the total torque at $i$ sample point. $T_{av}$ is the average total torque for $n$ points. $T_{\max}$ and $T_{\min}$ denote the maximum value and minimum value of the torque ripple. Table 5 shows the $T_{RC}$ for each method from experimental result, and Fig. 17 shows $T_{RC}$ and $T_{std}$ for each method with 10N · m load torque under different speed conditions.

According to Fig. 17, the proposed method can get better torque performance in steady state comparing to 12VVs DTC and optimized DITC. Fig. 18 shows the torque mutation waveform for each method when the load torque suddenly changed from 6N · m to 10N · m at 800rpm. From Fig. 18, obviously all these methods have good dynamic response because the torque is directly controlled, but the torque amplitude for proposed method is smaller than DTC and DITC.

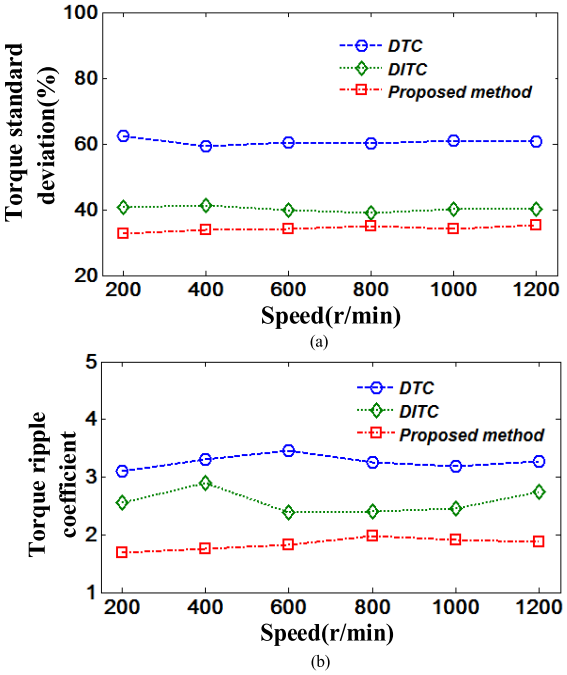


**FIGURE 17.** Evaluation for each method with 10N-m load. (a) Torque standard deviation. (b) Torque ripple coefficient.

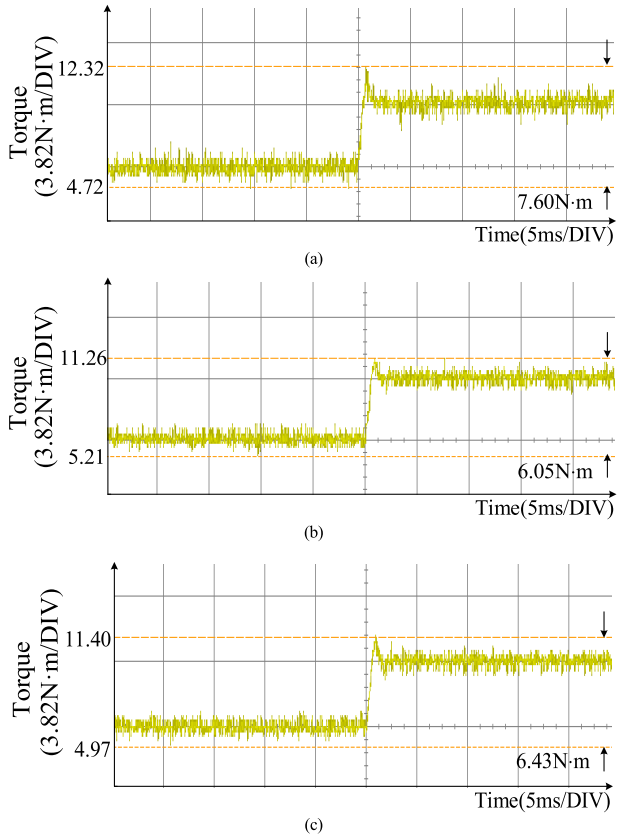


**FIGURE 18.** The torque mutation waveform. (a) DTC. (b) Proposed method. (c) DITC.

### C. SOME ADVICE AND ADDITIONAL THINKING

#### 1) NONLINEAR MODEL

Establishment of an accurate nonlinear model is prerequisite for MPC. For SRM's nonlinear model, many researchers have done a lot of work in this area [34]–[37]. Basically, the establishment of a nonlinear model is based on the magnetic flux characteristics of special positions. These methods all need the parameters obtained from locked rotor test. The higher the accuracy of the model, the more parameters are required. In general, the choice of the model needs to be traded off between practical and accurate. Another interesting stuff is that whether to establish the nonlinear model or execute locked rotor test, only one phase is under consideration, but there is no comprehensive information for whether and how the flux characteristics changes when multi-phase operate. This problem is a challenge for improving the MPC control strategy for SRM.

Recent years, compensating one step delay between selected voltage vectors and applied voltage vectors is under consideration for MPC applied on single-vector-based method [25], [26]. For SRM, the influence of this delay is not as much as IM or PMSM. first in SRM, the torque changes behind the flux, the proposed method predicts the flux at next period to control the torque in advance, this strategy can partly compensate this delay. Another reason is the accuracy of model, multi-step prediction requires more accurate mathematical model, if the model cannot achieve such accuracy, the result of multi-step prediction may get just the opposite. Also for the discrete method, the second order Runge-Kutta method or the other complex approaches could be adopted to reduce truncation error in consideration of different hardware environment.

#### 2) CONSTANT REFERENCE FLUX LINKAGE VALUE

Both DTC and proposed method need the reference flux linkage, and this value is constant in this paper. Some scholars indicate that the constant reference flux value is not suitable for all working conditions. Actually, from angle-flux curve, when the motor is running at high speed, the amplitude of given flux required for the running of SRM becomes smaller than before. Thus, with the increasing of speed, the given flux should be smaller in theory. But this change is really small (less than 0.01Wb). Thus, this influence can totally be overcome by setting the reference flux value under intermediate state. In this paper the reference flux is 0.33 Wb.

## VI. DEVELOPMENT PROSPECT

The DTC and DITC in this paper are further improved respectively. As the unique electromagnetic relationship in SRM leads flux hysteresis causes more error to the system, the development prospect for this method aims to refine the partition and increase the number of VVs just like 12VVs are adopted in this paper. Although DTC usually causes large torque ripple, simple structure and good robustness make this method still become one of the main algorithms for SRM.

For DITC, the main drawbacks are its large peak current and complicate hysteresis rules. For torque ripple, DITC is much smaller than other methods, but the turn on/off angle need to be optimized online from different conditions and this process needs lots of simulation and experimental tests.

since MPC is a promising method to handle the non-linear magnetic characteristic of SRM and avoids the complex switching rules, the proposed method could partly overcome some drawbacks for traditional SRM control. If the mathematical model for SRM could be simpler and precise in the future, the prospect for MPC used in SRM would be better.

## VII. CONCLUSION

Under the DTC scheme of SRM, a new method based on MPFC has been presented to reduce the torque ripple in this paper. Since the flux linkage hysteresis has been replaced by the cost function, the selection of voltage vectors can be more flexible to regulate the torque in advance. As the consideration of nonlinear electromagnetic characteristics, the new approach can partly overcome the torque ripple compared with the optimized DTC and DITC methods. Some advice and the possible improvement approaches for MPC used in SRM are also indicated in this paper. Simulation and experimental results are carried out in steady-state and dynamic-state to demonstrate the validity of the new control approach.

## REFERENCES

[1] K. Kiyota, T. Kakishima, and A. Chiba, "Comparison of test result and design stage prediction of switched reluctance motor competitive with 60-kW rare-earth PM motor," *IEEE Trans. Ind. Electron.*, vol. 61, no. 10, pp. 5712–5721, Oct. 2014.

[2] C. Gan, J. Wu, Q. Sun, W. Kong, H. Li, and Y. Hu, "A review on machine topologies and control techniques for low-noise switched reluctance motors in electric vehicle applications," *IEEE Access*, vol. 6, pp. 31430–31443, 2018.

[3] M. Ma, Z. Chang, Y. Hu, F. Li, C. Gan, and W. Cao, "An integrated switched reluctance motor drive topology with voltage-boosting and on-board charging capabilities for plug-in hybrid electric vehicles (PHEVs)," *IEEE Access*, vol. 6, pp. 1550–1559, 2018.

[4] K. Ha, C. Lee, J. Kim, R. Krishnan, and S. G. Oh, "Design and development of low-cost and high-efficiency variable-speed drive system with switched reluctance motor," *IEEE Trans. Ind. Appl.*, vol. 43, no. 3, pp. 703–713, May 2007.

[5] M. Takeno, A. Chiba, N. Hoshi, S. Ogasawara, M. Takemoto, and M. A. Rahman, "Test results and torque improvement of the 50-kW switched reluctance motor designed for hybrid electric vehicles," *IEEE Trans. Ind. Appl.*, vol. 48, no. 4, pp. 1327–1334, Jul. 2012.

[6] A. Chiba *et al.*, "Torque density and efficiency improvements of a switched reluctance motor without rare-earth material for hybrid vehicles," *IEEE Trans. Ind. Appl.*, vol. 47, no. 3, pp. 1240–1246, May/Jun. 2011.

[7] F. Peng, J. Ye, and A. Emadi, "A digital PWM current controller for switched reluctance motor drives," *IEEE Trans. Power Electron.*, vol. 31, no. 10, pp. 7087–7098, Oct. 2016.

[8] S. E. Schulz and K. M. Rahman, "High-performance digital PI current regulator for EV switched reluctance motor drives," *IEEE Trans. Ind. Appl.*, vol. 39, no. 4, pp. 1118–1126, Jul. 2003.

[9] R. Cardenas, R. Pena, M. Perez, J. Clare, G. Asher, and P. Wheeler, "Control of a switched reluctance generator for variable-speed wind energy applications," *IEEE Trans. Energy Convers.*, vol. 20, no. 4, pp. 781–791, Dec. 2005.

[10] J. Ye, B. Bilgin, and A. Emadi, "An offline torque sharing function for torque ripple reduction in switched reluctance motor drives," *IEEE Trans. Energy Convers.*, vol. 30, no. 2, pp. 726–735, Jun. 2015.

[11] X. D. Xue, K. W. E. Cheng, and S. L. Ho, "Optimization and evaluation of torque-sharing functions for torque ripple minimization in switched reluctance motor drives," *IEEE Trans. Power Electron.*, vol. 24, no. 9, pp. 2076–2090, Sep. 2009.

[12] V. P. Vujičić, "Minimization of torque ripple and copper losses in switched reluctance drive," *IEEE Trans. Power Electron.*, vol. 27, no. 1, pp. 388–399, Jan. 2012.

[13] P. C. Kjaer, J. J. Gribble, and T. J. E. Miller, "High-grade control of switched reluctance machines," *IEEE Trans. Ind. Appl.*, vol. 33, no. 6, pp. 1585–1593, Nov. 1997.

[14] I. Husain, "Minimization of torque ripple in SRM drives," *IEEE Trans. Ind. Electron.*, vol. 49, no. 1, pp. 28–39, Feb. 2002. doi: 10.1109/41.982245.

[15] R. B. Inderka and R. W. A. A. D. Doncker, "DITC-direct instantaneous torque control of switched reluctance drives," *IEEE Trans. Ind. Appl.*, vol. 39, no. 4, pp. 1046–1051, Jul. 2003.

[16] A. D. Cheok and Y. Fukuda, "A new torque and flux control method for switched reluctance motor drives," *IEEE Trans. Power Electron.*, vol. 17, no. 4, pp. 543–557, Jul. 2002.

[17] Q. Sun, J. Wu, C. Gan, M. Shen, and Y. Hu, "Investigation of direct torque control and torque sharing function strategy for switched reluctance motor applications," in *Proc. 18th Int. Conf. Elect. Mach. Syst. (ICEMS)*, Oct. 2015, pp. 864–868.

[18] V. Petrus, A.-C. Pop, C. S. Martis, V. Iancu, and J. Gyselinck, "Direct instantaneous torque control of SRMs versus current profiling—Comparison regarding torque ripple and copper losses," in *Proc. 13th Int. Conf. Optim. Elect. Electron. Equip. (OPTIM)*, May 2012, pp. 366–372.

[19] N. Yan, X. Cao, and Z. Deng, "Direct torque control for switched reluctance motor to obtain high torque–ampere ratio," *IEEE Trans. Ind. Electron.*, vol. 66, no. 7, pp. 5144–5152, Jul. 2019.

[20] S. Kouro, P. Cortes, R. Vargas, U. Ammann, and J. Rodriguez, "Model predictive control—A simple and powerful method to control power converters," *IEEE Trans. Ind. Electron.*, vol. 56, no. 6, pp. 1826–1838, Jun. 2009.

[21] J. Rodríguez *et al.*, "State of the art of finite control set model predictive control in power electronics," *IEEE Trans. Ind. Informat.*, vol. 9, no. 2, pp. 1003–1016, May 2013.

[22] F. Wang, S. Li, X. Mei, W. Xie, J. Rodríguez, and R. M. Kennel, "Model-based predictive direct control strategies for electrical drives: An experimental evaluation of PTC and PCC methods," *IEEE Trans. Ind. Informat.*, vol. 11, no. 3, pp. 671–681, Jun. 2015.

[23] Y. Zhang and H. Yang, "Model predictive torque control of induction motor drives with optimal duty cycle control," *IEEE Trans. Power Electron.*, vol. 29, no. 12, pp. 6593–6603, Dec. 2014.

[24] W. Xie *et al.*, "Finite-control-set model predictive torque control with a deadbeat solution for PMSM drives," *IEEE Trans. Ind. Electron.*, vol. 62, no. 9, pp. 5402–5410, Sep. 2015.

[25] X. Zhang and B. Hou, "Double vectors model predictive torque control without weighting factor based on voltage tracking error," *IEEE Trans. Power Electron.*, vol. 33, no. 3, pp. 2368–2380, Mar. 2018.

[26] Y. Zhang, Y. Bai, and H. Yang, "A universal multiple-vector-based model predictive control of induction motor drives," *IEEE Trans. Power Electron.*, vol. 33, no. 8, pp. 6957–6969, Aug. 2018.

[27] M. R. Nikzad, B. Asaei, and S. O. Ahmadi, "Discrete duty-cycle-control method for direct torque control of induction motor drives with model predictive solution," *IEEE Trans. Power Electron.*, vol. 33, no. 3, pp. 2317–2329, Mar. 2018.

[28] R. Mikail, I. Husain, Y. Sozer, M. S. Islam, and T. Sebastian, "A fixed switching frequency predictive current control method for switched reluctance machines," *IEEE Trans. Ind. Appl.*, vol. 50, no. 6, pp. 3717–3726, Nov./Dec. 2014.

[29] X. Li and P. Shamsi, "Inductance surface learning for model predictive current control of switched reluctance motors," *IEEE Trans. Transport. Electrific.*, vol. 1, no. 3, pp. 287–297, Oct. 2015.

[30] H. Le-Huy and P. Brunelle, "A versatile nonlinear switched reluctance motor model in Simulink using realistic and analytical magnetization characteristics," in *Proc. 31st Ann. Conf. IEEE Ind. Electron. Soc.*, Nov. 2005, pp. 1–6.

[31] F. Villarroel, J. R. Espinoza, C. A. Rojas, J. Rodríguez, M. Rivera, and D. Sbarbaro, "Multiobjective switching state selector for finite-states model predictive control based on fuzzy decision making in a matrix converter," *IEEE Trans. Ind. Electron.*, vol. 60, no. 2, pp. 589–599, Feb. 2013.

[32] P. Cortes *et al.*, "Guidelines for weighting factors design in model predictive control of power converters and drives," in *Proc. IEEE Int. Conf. Ind. Technol.*, Feb. 2009, pp. 1–7.

[33] S. A. Davari, D. A. Khaburi, and R. Kennel, "An improved FCS–MPC algorithm for an induction motor with an imposed optimized weighting factor," *IEEE Trans. Power Electron.*, vol. 27, no. 3, pp. 1540–1551, Mar. 2012.
[34] S. Song, M. Zhang, and L. Ge, "A new fast method for obtaining flux-linkage characteristics of SRM," *IEEE Trans. Ind. Electron.*, vol. 62, no. 7, pp. 4105–4117, Jul. 2015.
[35] H. P. Chi, R. L. Lin, and J. F. Chen, "Simplified flux-linkage model for switched-reluctance motors," *IEE Proc.-Electr. Power Appl.*, vol. 152, no. 3, pp. 577–583, May 2005.
[36] P. Zhang, P. A. Cassani, and S. S. Williamson, "An accurate inductance profile measurement technique for switched reluctance machines," *IEEE Trans. Ind. Electron.*, vol. 57, no. 9, pp. 2972–2979, Sep. 2010.
[37] L. Shen, J. Wu, S. Yang, and X. Huang, "Fast flux linkage measurement for switched reluctance motors excluding rotor clamping devices and position sensors," *IEEE Trans. Instrum. Meas.*, vol. 62, no. 1, pp. 185–191, Jan. 2013.
[38] R. Suryadevara and B. G. Fernandes, "Modified direct instantaneous torque control of switched reluctance motor with high torque per ampere and reduced source current ripple," in *Proc. Int. Power Electron. Conf. (IPEC)*, Hiroshima, Japan, May 2014, pp. 2433–2437.

**AIDE XU** received the B.S. degree in electric traction and transmission control from Dalian Jiaotong University, Dalian, China, in 1997, and the M.S. degree in power electronics and power drives and the Ph.D. degree in marine engineering from Dalian Maritime University, Dalian, in 2003 and 2010, respectively. She was a Lecturer and an Associate Professor with Dalian Maritime University, from 2003 to 2014, where she has been a Professor with the Department of Electrical Engineering, Faculty of College of Information Science and Technology, since 2015. Her research interests include motion control and motor drives.

**CHAOYI SHANG** was born in Qingdao, China, in 1995. He received the B.S. degree in electronic and electrical engineering from Jimei University, Xiamen, in 2017. He is currently pursuing the M.S. degree in electrical engineering with Dalian Maritime University.

His research interests include control strategy for non-linear systems and treatment of data.

**JIAGUI CHEN** was born in Zunyi, China, in 1993. He received the B.S. degree in electronic science and technology from Dalian Jiaotong University, Dalian, in 2017. He is currently pursuing the M.S. degree in electronic science and technology with Dalian Maritime University.

His research interest includes switched reluctance motors and their controls, particularly for the sensorless control of the motor systems.

**JINGWEI ZHU** received the B.S. degree in automation instrumentation engineering from the Jinzhou Institute of Technology, Jinzhou, China, in 1985, the M.S. degree in electronic engineering from the Shenyang University of Technology, Shenyang, China, in 1990, and the Ph.D. degree in electrical engineering from Adelaide University, Adelaide, Australia, in 2008.

He was a Lecturer and an Associate Professor with the Jinzhou Institute of Technology, from 1985 to 1999. In 2000, he joined the Marine Electrical Engineering College, Dalian Maritime University, China, where he is currently a Professor. His research interests include design and control for electrical machine systems, power electronic devices, and sustainable energy generation.

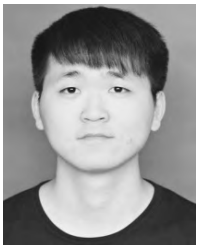

**LELE HAN** received the B.S. degree in electronic information engineering from Anhui Normal University, Anhui, China, in 2017. He is currently pursuing the M.S. degree with the College of Information Science and Technology, Dalian Maritime University, Dalian, China.

His research interest includes neural networks and control in switched reluctance motors, particularly for the optimization of the torque ripple and efficiency of the motor systems.